A SECOND-ORDER TIME ACCURATE FINITE ELEMENT FORMULATION FOR QUASI-INCOMPRESSIBLE VISCOUS FLOW AND HEAT TRANSFER STABILIZED BY LOCAL TIME-STEPS

Curi, M.F., mfcuri@ien.gov.br
De Sampaio, P.A.B., sampaio@ien.gov.br
Nuclear Engineering Institute/CNEN, P.O. Box 68550, Rio de Janeiro, RJ 21945-970, Brazil

Gonçalves Jr, M.A., milton.a.g.j@gmail.com
Center for Parallel Computations, Federal University of Rio de Janeiro, P.O. Box 68516, Rio de Janeiro, RJ 21945-970, Brazil

Abstract. *A stabilized finite element method for the solution of viscous flow and heat transfer is presented. An equation for pressure is derived from a second-order time accurate Taylor-Galerkin procedure that combines the mass and the momentum conservation laws. At each time-step, once the pressure has been determined, the velocity field and the temperature field are computed solving discretized equations obtained from another second-order time accurate scheme and a least-squares minimization of momentum and energy residual. Thus, the procedure leads to a stabilized finite element method suitable for the simulation of heat transfer problems in free, mixed and forced convection. The terms that stabilize the finite element method arise naturally from the process, rather than being introduced a priori in the variational formulation. Local time-steps, chosen according to the time-scales of convection-difusion of momentum and energy, play the role of stabilization parameters. Numerical solutions of some representative examples demonstrate the application of the proposed stabilized formulation, where good agreement with previously published experimental and computational results have been obtained.*

Keywords*: Finite element method, computational fluid dynamic, stabilized finite element method, incompressible viscous flows and heat transfer, second-order time accurate methods*

1. Introduction

A number of stabilized finite element formulations have been proposed to overcome the deficiencies of the standard Galerkin method when applied to fluid dynamics. Such formulations have been successful in dealing with convection-dominated problems and also with the incompressibility constraint in incompressible viscous flows. Indeed, stabilized formulations permit controlling the wiggles in the simulation of convective problems. They also permit circumventing the Babuška-Brezzi restrictions (Brezzi and Fortin, 1991) on the choice of the interpolation spaces in the approximation of the incompressible Navier–Stokes equations written in primitive variables. The stabilized formulation presented avoids this difficulty through the introduction of extra stabilizing terms (De Sampaio, 1991, 1993; De Sampaio and Coutinho, 1999).

Stabilized finite element formulations comprise the standard Galerkin approximation plus extra terms responsible for enhancing stability. Whilst the extra terms contribute to stabilize the method, they do not affect consistency, as they tend to zero for vanishing discretization residuals. The stabilized formulations can be often interpreted as Petrov–Galerkin weighted residual approximations, where the usual Galerkin weighting function is modified with the addition of a perturbation. The terms resulting from the interaction of the perturbation with the residual generate the desired stabilization effect, without compromising the consistency of the approximation. For stabilization formulations details see De Sampaio (1991, 2005, 2006).

In order to introduce the correct amount of stabilization everywhere on the domain of analysis, the time-step must be defined locally, leading to spatially varying time-step distributions. The procedure proposed in De Sampaio (2006) is followed. In this case the use of local time-steps and the required synchronization scheme are embedded in the method. The result is a method that resembles well known stabilized formulations that employ a single time-step for the whole domain and a local definition of stabilization parameters, but whose origins are based on the use of local time-steps combined with a synchronization scheme.

In this work a finite element method for quasi-incompressible viscous flows and heat transfer is presented. As in the previous works mentioned above, the time discretization precedes the spatial discretization. However, here the time discretizations employed are improved to second order accuracy. In the present method an equation for pressure is derived from a second-order time accurate Taylor-Galerkin procedure that combines the mass and the momentum conservation laws.

At each time-step, once the pressure has been determined, the velocity and temperature fields are computed solving discretized equations obtained from another second-order time accurate scheme and a least-squares minimization of spatial momentum and energy residuals. The terms that stabilize the finite element method (controlling wiggles and circumventing the Babuška-Brezzi condition) arise naturally from the process, rather than being introduced a priori in the variational formulation. The method demonstrated good agreement with previously published experimental and computational results.

2. Physical Model

We consider a continuum model for quasi-incompressible viscous flows including buoyancy forces and heat transfer. The problem is defined on the open bounded domain Ω, with boundary Γ, contained in nsd-dimensional Euclidean space. The flow is governed by the quasi-incompressible Navier-Stokes equations and an energy convection-diffusion equation. These are written using the summation convention for *a=1,2,...,nsd e b=1,2,...,nsd,* in Cartesian coordinates:

$$\rho\left[\frac{\partial u_a}{\partial t}+u_b\frac{\partial u_a}{\partial x_b}\right]-\frac{\partial \tau_{ab}}{\partial x_b}+\frac{\partial p}{\partial x_a}+\rho\beta g_a\left(T-T_0\right)=0 \tag{1}$$

$$\frac{1}{\rho c_s{}^2}\frac{\partial p}{\partial t}+\frac{\partial u_a}{\partial x_a}=0 \tag{2}$$

$$\rho c\left[\frac{\partial T}{\partial t}+u_b\frac{\partial T}{\partial x_b}\right]+\frac{\partial q_b}{\partial x_b}=0 \tag{3}$$

The dependent variables are the velocity, pressure and temperature fields represented by u_a, p and T, respectively. The sound speed is denoted by c_s. The fluid specific heat is represented by c. Note that the viscous stress is given by $\tau_{ab}=\mu\left(\partial u_a/\partial x_b+\partial u_b/\partial x_a\right)$, where μ is the fluid viscosity. The heat flux is given by $q_b=-\kappa\,\partial T/\partial x_b$, where κ is the fluid thermal conductivity. The fluid density (at the reference temperature T_0) is denoted by ρ. The volumetric expansion coefficient of the fluid is $\beta=-\rho^{-1}\,\partial\rho/\partial T$

Velocity and traction boundary conditions are prescribed by given data on non-overlapping boundary partitions Γ_{ua} and Γ_{ta}, such that $\Gamma_{ua}\bigcup\Gamma_{ta}=\Gamma$, according to:

$$u_a=\overline{u_a}(\mathbf{x},t),\qquad \mathbf{x}\in\Gamma_{ua}, \tag{4}$$

$$\left(-p\delta_{ab}+\tau_{ab}\right)n_b=\overline{t_a}(\mathbf{x},t),\qquad \mathbf{x}\in\Gamma_{ta}, \tag{5}$$

where δ_{ab} is the Kronecker delta and n_b denotes Cartesian components of the outward normal vector at the boundary.

Temperature and heat flux boundary conditions are prescribed by given data on non-overlapping boundary partitions Γ_T and Γ_q, such that $\Gamma_T\bigcup\Gamma_q=\Gamma$, according to:

$$T=\overline{T}(\mathbf{x},t),\qquad \mathbf{x}\in\Gamma_T, \tag{6}$$

$$q_bn_b=\overline{q}(\mathbf{x},t),\qquad \mathbf{x}\in\Gamma_q, \tag{7}$$

Pressure and normal velocity conditions are prescribed by given data on non-overlapping boundary partitions Γ_p and Γ_G, such that $\Gamma_p\bigcup\Gamma_G=\Gamma$, according to:

$$p=\overline{p}(\mathbf{x},t),\qquad \mathbf{x}\in\Gamma_p, \tag{8}$$

$$u_bn_b=\overline{G}(\mathbf{x},t),\qquad \mathbf{x}\in\Gamma_G. \tag{9}$$

2.1. Governing equations in non-dimensional form

Here the variables are non-dimensionalized with respect to reference scales conveniently chosen from the problem data. The non-dimensional velocity, pressure and temperature are represented by $u'_a=u_a/u_0$, $p'=p/\rho u_0^2$ and $T'=\left(T-T_0\right)/\left(T_{\max}-T_{\min}\right)$, respectively. Note that u_0 is the velocity reference scale and $T_{\max}$ and $T_{\min}$ are the

maximum and minimum temperatures in the problem. The spatial co-ordinates are non-dimensionalized with respect to the reference length L, i.e., $x'_a = x_a / L$. The non-dimensional time is represented by $t' = t\,u_0 / L$. The gravity field is non-dimensionalized with respect to its modulus $g'_a = g_a / \|\mathbf{g}\|$.

In terms of the non-dimensional variables the governing equations become:

$$\frac{\partial u'_a}{\partial t'} + u'_b \frac{\partial u'_a}{\partial x'_b} - \frac{1}{Re}\frac{\partial}{\partial x'_b}\left(\frac{\partial u'_a}{\partial x'_b} + \frac{\partial u'_b}{\partial x'_a}\right) + \frac{\partial p'}{\partial x'_a} + Rig'_a T' = 0 \tag{10}$$

$$M^2 \frac{\partial p'}{\partial t'} + \frac{\partial u'_a}{\partial x'_a} = 0 \tag{11}$$

$$\frac{\partial T'}{\partial t'} + u'_b \frac{\partial T'}{\partial x'_b} - \frac{1}{RePr}\frac{\partial}{\partial x'_b}\left(\frac{\partial T'}{\partial x'_b}\right) = 0 \tag{12}$$

where $M = u_0 / c_s$ is the Mach number, $Re = \rho\|\mathbf{u}\|L/\mu$ is the Reynolds number, $Ri = \beta(T_{\max} - T_{\min})\|\mathbf{g}\|L/u_0^2$ is the Richardson number, $Pr = c\mu/\kappa$ is the Prandtl number.

The non-dimensional form used in Eq. (10), Eq.(11) and Eq.(12) is suitable for mixed and forced convection flows, where a reference velocity is generally available from the problem data. However, this is not the case for free convection, for which we have to obtain the velocity time scale indirectly, defining it as $u_0 = \sqrt{\beta(T_{\max} - T_{\min})\|\mathbf{g}\|L}$. Thus, for free convection, the Reynolds and Richardson numbers that appear in the non-dimensional equations become $Ri = 1$ and $Re = \sqrt{Ra/Pr}$, respectively, where $Ra = \rho^2 c\|\mathbf{g}\|\beta(T_{\max} - T_{\min})L^3/\mu\kappa$ is the Rayleigh number. The non-dimensional boundary conditions remain the same forms presented previously.

3. **Stable Finite Element Formulation**

In this paper we use these non-dimensional equations, thus the superscript " ' " used to denote the non-dimensional quantities will be dropped.

3.1.**Pressure equation**

To obtain an equation for pressure update, we use a Taylor series for pressure in time. Thus, from this Taylor series we have:

$$\frac{p^{n+1} - p^n}{\Delta t} = \frac{\partial p^n}{\partial t} + \frac{\Delta t}{2}\frac{\partial}{\partial t}\left(\frac{\partial p}{\partial t}\right)^{n+\theta} + 0\left(\Delta t^2\right) \tag{13}$$

where $0 \le \theta \le 1$. The superscript n e $n+1$ indicates the time level and Δt indicates the time step. The pressure change during the time step Δt is represented by $\Delta p = p^{n+1} - p^n$.

Substituting the mass balance, given by Eq. (11) in Eq. (13), followed by the introduction of the momentum balance given by Eq. (10), we obtain the following (see Gonçalves Jr. and De Sampaio, 2010):

$$M^2 \frac{\Delta p}{\Delta t} - \frac{\Delta t}{2}\frac{\partial}{\partial x_a}\left(\frac{\partial \Delta p}{\partial x_a}\right) = \left[-\frac{\partial u_a}{\partial x_a} + \frac{\Delta t}{2}\frac{\partial}{\partial x_a}\left(u_b \frac{\partial u_a}{\partial x_b} - \left(\frac{\partial \tau_{ab}}{\partial x_b}\right) + \frac{\partial p}{\partial x_a} + Rig_a T \right)\right]^n + 0\left(\Delta t^2\right) \tag{14}$$

The spatial discretization is performed with Lagrangian linear triangular elements in 2D. For the problem variables, we have: $\hat{u}_a^n = N_j u_{aj}^n$, $\hat{T}^n = N_j T_j^n$, $\hat{p}^n = N_j p_j^n$, and $\Delta\hat{p}^n = N_j \Delta p_j$. Note that N_j represents the shape functions of the finite element and the variables with the subscript j are nodal values.

Employing the classical Galerkin method, using Green's identity to Eq. (14), and introducing the boundary conditions given by Eq. (9), we obtain:

$$\int_\Omega M^2 N_i \frac{\Delta\hat{p}}{\Delta t} d\Omega + \int_\Omega \frac{\Delta t}{2}\frac{\partial N_i}{\partial x_a}\frac{\partial \Delta\hat{p}}{\partial x_a} d\Omega = -\int_\Omega N_i \frac{\partial \hat{u}_a^n}{\partial x_a} d\Omega - \int_\Omega \frac{\Delta t}{2}\frac{\partial N_i}{\partial x_a}\left[\hat{u}_b^n \frac{\partial \hat{u}_a^n}{\partial x_b} + \frac{\partial \hat{p}^n}{\partial x_a} + Rig_a \hat{T}^n \right] - \int_{\Gamma_G} \frac{N_i}{2}\left(\overline{G}^{n+1} - \overline{G}^n\right) d\Gamma \tag{15}$$

Once again, mathematical details are explored in Gonçalves Jr. and De Sampaio (2010). Substituting $\Delta\hat{p} = N_j \Delta p_j$ in Eq. (15), obtain a symmetric equation system for calculating the nodal values of the pressure update:

$$\left[\mathbf{A_{pp_{ij}}}\right]\left\{\mathbf{\Delta p_j}\right\} = \left\{\mathbf{F_{p_i}}\right\} \tag{16}$$

3.2.Velocity and Temperature equations

Once the pressure field has been determined, we use a second order accurate time discretization for the momentum and energy balance given by Eq. (10) and Eq. (12) to obtain equations for the velocity and temperature update.

Discretizations of Eq. (10) and Eq. (12) with respect to time are given by:

$$\frac{\Delta u_a}{\Delta t_M} + \frac{1}{2}\left(u_b^n \frac{\partial \Delta u_a}{\partial x_b} + \Delta u_b \frac{\partial u_a^n}{\partial x_b} \right) - \frac{1}{2Re}\frac{\partial}{\partial x_b}\left(\frac{\partial \Delta u_a}{\partial x_b} + \frac{\partial \Delta u_b}{\partial x_a} \right) + \frac{Rig_a \Delta T}{2} = -\left[u_b^n \frac{\partial u_a^n}{\partial x_b} + \frac{\partial p^{n+1/2}}{\partial x_a} - \frac{\partial \tau_{ab}^n}{\partial x_b} + Rig_a T^n \right] + 0\left(\Delta t^2\right) \tag{17}$$

$$\frac{\Delta T}{\Delta t_E} + \frac{1}{2}\left(u_b^n \frac{\partial \Delta T}{\partial x_b} + \Delta u_b \frac{\partial T^n}{\partial x_b} \right) - \frac{1}{2RePr}\frac{\partial}{\partial x_b}\left(\frac{\partial \Delta T}{\partial x_b} \right) = -\left[u_b^n \frac{\partial T^n}{\partial x_b} + \frac{\partial q_b^n}{\partial x_b} \right] + 0\left(\Delta t^2\right) \tag{18}$$

As mentioned earlier, the superscript n e $n+1$ indicates the time level and Δt denotes the time step. The velocity change during the time step Δt_M is represented by $\Delta u_a = u_a^{n+1} - u_a^n$. The temperature change during the time step Δt_E is $\Delta T = T^{n+1} - T^n$. The pressure field at time level $n+1/2$ is written as $p^{n+1/2} = p^n + \Delta p/2$.

Consider the following spatial discretization of the problem variables: $\hat{u}_a^n = N_j u_{aj}^n$, $\Delta\hat{u}_a = N_j \Delta u_{aj}$, $\hat{T}^n = N_j T_j^n$ and $\Delta\hat{T} = N_j \Delta T_j$. Again, N_j represents the shape functions of the finite element and the variables with the subscript j are nodal values. Using the discretized field of variables, we can write the following expressions for the squared discretization residuals of Equation. (17 and 18):

$$\Pi = \int_\Omega \lambda \hat{R}_a \hat{R}_a d\Omega + \int_\Omega \xi \hat{E}\hat{E} d\Omega \tag{19}$$

where λ e ξ are a scaling parameters to be defined later and $\hat{R}_a$ and $\hat{E}$ are discretization residuals of Eq. (17) and Eq. (18), and written as::

$$\hat{R}_a = \frac{1}{\Delta t_M}\left[\Delta\hat{u}_a + \frac{\Delta t_M}{2}\left(\hat{u}_b^n \frac{\partial \Delta\hat{u}_a}{\partial x_b} + \Delta\hat{u}_b \frac{\partial \hat{u}_a^n}{\partial x_b} \right) \right] - \frac{1}{2Re}\frac{\partial}{\partial x_b}\left(\frac{\partial \Delta\hat{u}_a}{\partial x_b} + \frac{\partial \Delta\hat{u}_b}{\partial x_a} \right) + \frac{Rig_a \Delta\hat{T}}{2} + \left[\hat{u}_b^n \frac{\partial \hat{u}_a^n}{\partial x_b} + \frac{\partial \hat{p}^{n+1/2}}{\partial x_a} - \frac{\partial \hat{\tau}_{ab}^n}{\partial x_b} + Rig_a \hat{T}^n \right] \tag{20}$$

$$\hat{E} = \frac{1}{\Delta t_E}\left[\Delta\hat{T} + \frac{\Delta t_E}{2}\left(\hat{u}_b^n \frac{\partial \Delta\hat{T}}{\partial x_b} + \Delta\hat{u}_b \frac{\partial \hat{T}^n}{\partial x_b} \right) \right] - \frac{1}{2RePr}\frac{\partial}{\partial x_b}\left(\frac{\partial \Delta\hat{T}}{\partial x_b} \right) - \left[\hat{u}_b^n \frac{\partial \hat{T}^n}{\partial x_b} + \frac{\partial \hat{q}_b^n}{\partial x_b} \right] \tag{21}$$

Minimizing Π, given by Eq. (19), with respect to the free Δu_{ci} and free ΔT_i nodal values we get:

$$\int_\Omega \left[N_i + \frac{\Delta t_M}{2}\hat{u}_b^n \frac{\partial N_i}{\partial x_b} \right] \hat{R}_c d\Omega + \int_\Omega \frac{\Delta t_M}{2}\frac{\partial \hat{u}_a^n}{\partial x_c} N_i \hat{R}_a d\Omega + \int_\Omega \frac{\Delta t_E}{2}\frac{\partial \hat{T}^n}{\partial x_c} N_i \hat{E} d\Omega = 0 \qquad \forall \text{ free } \Delta u_{ci} \tag{22}$$

$$\int_\Omega \left[N_i + \frac{\Delta t_E}{2}\hat{u}_b^n \frac{\partial N_i}{\partial x_b} \right] \hat{E} d\Omega + \int_\Omega \frac{\Delta t_M}{2} R_i g_a N_i \hat{R}_a d\Omega = 0 \qquad \forall \text{ free } \Delta T_i \tag{23}$$

The parameters λ e ξ have been chosen as Δt_M e Δt_E respectively, in order to normalize (and non-dimensionalized) the weight functions in Equations (22 and 23).

Note that the weight functions present in the first terms of these Eqs. (22 and 23) have the same structure as the SUPG weight function method of Brooks and Hughes (1982). The remaining weight functions, affecting the second and third term in Eq. (22) and affecting the second term in Eq. (23), are specific of the method presented here.

Combining Eq. (22) and traction boundary condition, given by Eq. (5), we obtain the following discretized equations:

$$\int_\Omega \left[N_i + \frac{\Delta t_M}{2} \hat{u}_b^n \frac{\partial N_i}{\partial x_b} \right] \hat{R}_c d\Omega + \int_\Omega \frac{\Delta t_M}{2} \frac{\partial \hat{u}_a^n}{\partial x_c} N_i \hat{R}_a d\Omega + \int_\Omega \frac{\Delta t_E}{2} \frac{\partial \hat{T}^n}{\partial x_c} N_i \hat{E} d\Omega + \int_{\Gamma_{t_c}} N_i \left[\left(-p\delta_{cb} + \tau_{cb} \right) n_b - \bar{t}_c(\mathbf{x},t) \right]^{n+1/2} d\Gamma = 0 \quad \forall \text{ free } \Delta u_{ci} \tag{24}$$

$$\int_\Omega \left[N_i + \frac{\Delta t_E}{2} \hat{u}_b^n \frac{\partial N_i}{\partial x_b} \right] \hat{E} d\Omega + \int_\Omega \frac{\Delta t_M}{2} R_i g_a N_i \hat{R}_a d\Omega + \int_{\Gamma_q} N_i \left[q(\mathbf{x},t) - q_b n_b \right]^{n+1/2} d\Gamma = 0 \qquad \forall \text{ free } \Delta T_i \tag{25}$$

Again, a previous work explored the mathematical details (Gonçalves Jr. and De Sampaio, 2010). By introducing Eqs. (20 and 21) in Eqs. (24 and 25), using Green's identity, and replacing the problem variables: $\Delta \hat{u}_a = N_j \Delta u_{aj}$ and $\Delta \hat{T} = N_j \Delta T_j$ in Eqs. (24 and 25) we obtain a symmetric equation system to solve for the nodal values of velocity and temperature update. For 2D problems, we have the following system:

$$\begin{bmatrix} \mathbf{A_{uu\,ij}} & \mathbf{A_{uv\,ij}} & \mathbf{A_{uT\,ij}} \\ \mathbf{A_{uv\,ij}^T} & \mathbf{A_{vv\,ij}} & \mathbf{A_{vT\,ij}} \\ \mathbf{A_{uT\,ij}^T} & \mathbf{A_{vT\,ij}^T} & \mathbf{A_{TT\,ij}} \end{bmatrix} \begin{Bmatrix} \mathbf{\Delta u_j} \\ \mathbf{\Delta v_j} \\ \mathbf{\Delta T_j} \end{Bmatrix} = \begin{Bmatrix} \mathbf{F_{u\,i}} \\ \mathbf{F_{v\,i}} \\ \mathbf{F_{T\,i}} \end{Bmatrix} \tag{26}$$

It is important to note that the time-discretization is performed before the spatial discretization, which is performed using standard finite elements C_0. The terms multiplied by Δt_M and Δt_E in Eqs. (24 and 25) are responsible for controlling the spatial oscillations (wiggles) in convection-dominated flows, and stabilize the computation, regardless of the restrictions Babuška-Brezzi on the choice of interpolation spaces for velocity and temperature. In particular, the use of the equal order of interpolation for all variables adopted here become possible through a proper choice of Δt_M and Δt_E. It is important to remark that rather than being proposed a priori, the stabilization terms appear naturally in this method from least squares minimization of the time-discretized momentum and energy square residuals with respect to the temperature and velocity degrees of freedom (with free nodal values).

3.3 Local time-steps and synchronization

In this paper we propose an alternative way to choose the time step. Instead of using the method proposed by De Sampaio (1991, 1993, 2005) we chose the time step according to the minimum values of the characteristic time scales of convection and diffusion , i.e., $\Delta t_M = \min(t_c, t_{dM})$ and $\Delta t_E = \min(t_c, t_{dE})$, where $td_M = \rho h_e^{\,2} / 6\mu$ and $td_E = \rho h_e^{\,2} / 6\kappa$, are the momentum and energy diffusion time-scales respectively, and $tc = h_e / \left\| \mathbf{u}^n \right\|$ is the convection time scale. Here h_e is the mesh with local size (De Sampaio, 1991).

Because we have optimal time-steps that vary with position and according to the quantity transported (momentum or energy), we have to resort to a special scheme to synchronize the time advance of the computation. In this paper, we adopt the procedure introduced in De Sampaio (2006). It is based on selecting a synchronization time-step Δt^*, which will be the same for all flow variables and for all domain (in fact, the usual concept for a time-step).

The synchronization time-step is chosen to be quite close to the minimum problem time-step and is calculated as $\Delta t^* = 0.999 \min(\Delta t_M, \Delta t_E)$. The time-step Δt^* is the time step used for synchronizing the advancement of the numerical simulation. Let $\Delta \hat{u}_a$, $\Delta \hat{p}$ and $\Delta \hat{T}$ be the variable changes obtained when using the appropriate local time-steps to solve Eqs. (16 and 26). On the other hand, let us denote the variable changes from time t^n to the time $t^n + \Delta t^*$ (the synchronization time) as $\Delta \hat{u}_a^*$, $\Delta \hat{p}^*$ e $\Delta \hat{T}^*$. Thus, keeping the same rate of change, we have the following relations:

$$\frac{\Delta\hat{u}_a^*}{\Delta t^*} = \frac{\Delta\hat{u}_a}{\Delta t_M} \tag{27}$$

$$\frac{\Delta\hat{p}^*}{\Delta t^*} = \frac{\Delta\hat{p}}{\Delta t_M} \tag{28}$$

$$\frac{\Delta\hat{T}^*}{\Delta t^*} = \frac{\Delta\hat{T}}{\Delta t_E} \tag{29}$$

where $\Delta\hat{u}_a^* = \hat{u}_a\left(\mathbf{x}, t^n + \Delta t^*\right) - \hat{u}_a\left(\mathbf{x}, t^n\right)$, $\Delta\hat{u}_a = \hat{u}_a\left(\mathbf{x}, t^n + \Delta t_M\right) - \hat{u}_a\left(\mathbf{x}, t^n\right)$, $\Delta\hat{p}^* = \hat{p}\left(\mathbf{x}, t^n + \Delta t^*\right) - \hat{p}\left(\mathbf{x}, t^n\right)$, $\Delta\hat{p} = \hat{p}\left(\mathbf{x}, t^n + \Delta t_M\right) - \hat{p}\left(\mathbf{x}, t^n\right)$, $\Delta\hat{T}^* = \hat{T}\left(\mathbf{x}, t^n + \Delta t^*\right) - \hat{T}\left(\mathbf{x}, t^n\right)$, and $\Delta\hat{T} = \hat{T}\left(\mathbf{x}, t^n + \Delta t_E\right) - \hat{T}\left(\mathbf{x}, t^n\right)$.

In practice, the computation based on local time-steps and the synchronization phase does not have to be performed separately. The the synchronization phase, represented by Eqs.(27, 28 and 29), can be embedded in Equations (16 and 26). Thus, the synchronized solution at $t^n + \Delta t^*$ can be obtained directly solving the following symmetric equations:

$$\left[\mathbf{A}^*_{\mathbf{pp_{ij}}}\right]\left\{\Delta\mathbf{p}^*_{\mathbf{j}}\right\} = \left\{\mathbf{F}_{\mathbf{p_i}}\right\} \tag{30}$$

$$\begin{bmatrix} \mathbf{A}^*_{\mathbf{uu_{ij}}} & \mathbf{A}^*_{\mathbf{uv_{ij}}} & \mathbf{A}^*_{\mathbf{uT_{ij}}} \\ \mathbf{A}^{*\mathbf{T}}_{\mathbf{uv_{ij}}} & \mathbf{A}^*_{\mathbf{vv_{ij}}} & \mathbf{A}^*_{\mathbf{vT_{ij}}} \\ \mathbf{A}^{*\mathbf{T}}_{\mathbf{uT_{ij}}} & \mathbf{A}^{*\mathbf{T}}_{\mathbf{vT_{ij}}} & \mathbf{A}^*_{\mathbf{TT_{ij}}} \end{bmatrix} \begin{Bmatrix} \Delta\mathbf{u}^*_{\mathbf{j}} \\ \Delta\mathbf{v}^*_{\mathbf{j}} \\ \Delta\mathbf{T}^*_{\mathbf{j}} \end{Bmatrix} = \begin{Bmatrix} \mathbf{F}_{\mathbf{u_i}} \\ \mathbf{F}_{\mathbf{v_i}} \\ \mathbf{F}_{\mathbf{T_i}} \end{Bmatrix} \tag{31}$$

The solution procedure is semi-segregated., in the sense that pressure is computed first and independently at each step but the solution of the velocity components and temperature are coupled, as shown in Equation (31). After each step the problem variables are updated and the computation proceeds until the specified final analysis time is reached.

All equation systems in the present formulation involve symmetric positive-definite matrices. The equation system is solved using the conjugate gradient method with Jacobi pre-conditioner, in an Element-by-Element (EBE) implementation. The computer code used here was developed for the study of 2D problems, where linear triangles were used to interpolate all dependent variables. The code also uses dynamic adaptive finite element meshes generated using Bowyer's algorithm (Bowyer, 1981), guided by the error estimation of Zienkiewicz and Zhu (1987).Was also employed parallel programming optimized for high performance on distributed parallel computing systems.

4. Numerical Examples

4.1. Free Convection in a Square Cavity

We consider a square cavity centered on *x=0* and *y=0* with length L (reference spatial scale), thermally insulated at the top and bottom walls. A reference pressure $p = 0$ is imposed at the center of the cavity. Non-slip velocity boundary conditions are imposed on all walls. The cavity contains a fluid that is initially at rest at temperature T_0. The left wall temperature is $T = T_0 + \Delta T/2$ and the right is at temperature $T = T_0 - \Delta T/2$. These boundary conditions at opposite parallel walls generate a free convection flow inside the cavity and, for sufficiently high Rayleigh numbers, thermal stratification occurs.

The numerical results are parameterized with respect to the Prandtl and Rayleigh numbers. We have performed numerical simulations at $Ra = 10^4$, $Ra = 10^5$ and $Ra = 10^6$. In all examples the Prandtl number was $Pr = 0.71$, with minimum element size of $0.005L$. The transients ran from $t = 0$ to $t = 60L/u_0$, where $u_0 = \sqrt{\beta(T_{\max} - T_{\min})\|\mathbf{g}\|L}$. In all cases this has been long enough to obtain convergence to steady-state.

Figure 1 presents the heat flux distribution at the left (hot) wall in terms of the Nusselt number. Note that the Nusselt number is given by $Nu = q_w L/\kappa(T_{\max} - T_{\min})$, where q_w is the local wall heat flux.

Table 1 compares our results for the mean and maximum Nusselt numbers with the benchmark provided by Hortmann *et al*. (1990). The use of adaptive meshes in our computations allowed obtaining results that agree within less than 0.19% with the benchmark data using much finer meshes.

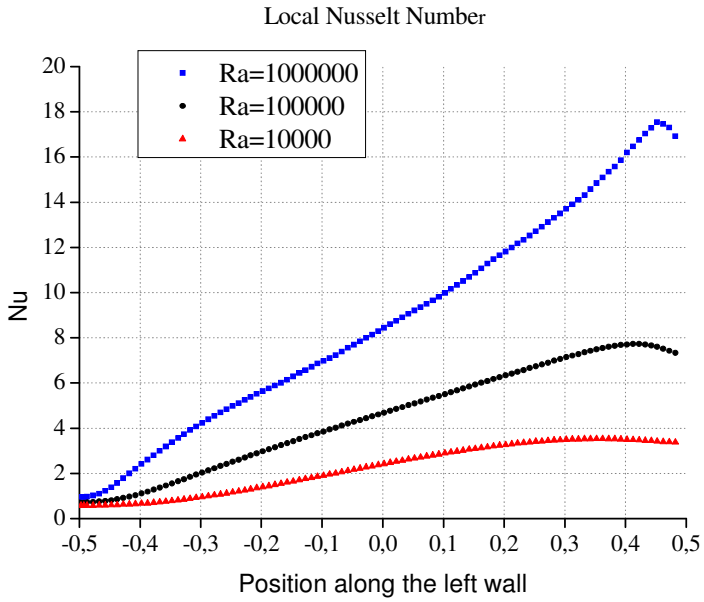

Figure 1: Local Nusselt number along the left (hot) wall for $Pr = 0.71$ and $Ra = 10^4$, $Ra = 10^5$ and $Ra = 10^6$

Figure 2 presents the final adaptive mesh, temperature field and pressure field for $Ra = 10^4$ and $Pr = 0.71$. The final adaptive mesh comprises 9574 nodes and 18346 elements. Figure 3 presents the final adaptive mesh, temperature field and pressure field for $Ra = 10^5$ and $Pr = 0.71$. The final adaptive mesh shows 7357 nodes and 13912 elements. Figure 4 presents the final adaptive mesh, temperature field and pressure field for $Ra = 10^6$ and $Pr = 0.71$. The final adaptive mesh comprises 6008 nodes and 11214 elements.

	$Ra = 10^4$ *Nu* max.	$Ra = 10^4$ *Nu* mean	$Ra = 10^5$ *Nu* max.	$Ra = 10^5$ *Nu* mean	$Ra = 10^6$ *Nu* max.	$Ra = 10^6$ *Nu* mean
Hortmann *et al.* (1990)	3.53087	2.24475	7.72013	4.52164	17.53600	8.82513
Present method	3.52976	2.24369	7.72337	4.51965	17.52739	8.80794

Table 1: Mean and maximum Nusselt numbers: comparison between the present results with those of Hortmann *et al.* (1990)

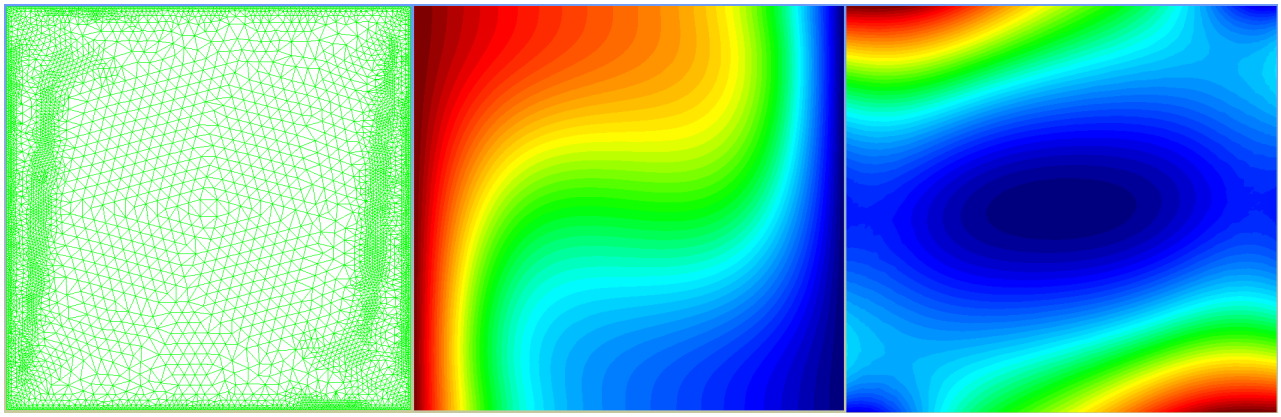

Figure 2: Adaptive mesh, temperature field and pressure field for $Ra = 10^4$ and $Pr = 0.71$

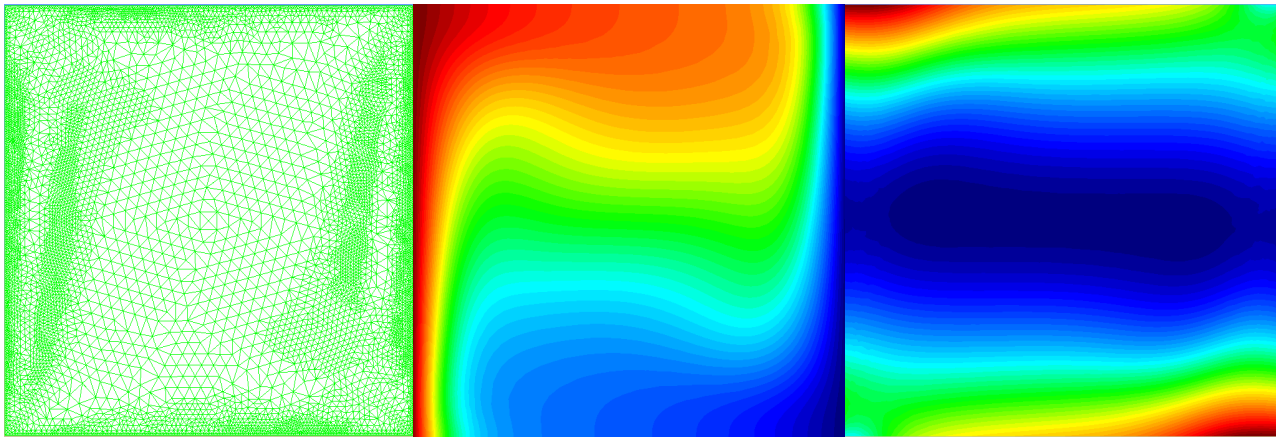

Figure 3: Adaptive mesh, temperature field and pressure field for $Ra = 10^5$ and $Pr = 0.71$

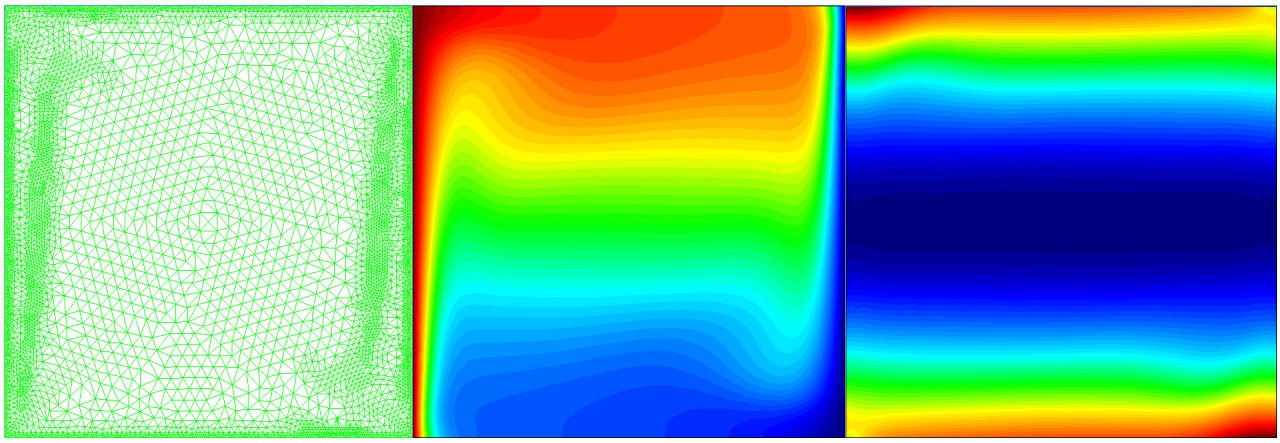

Figure 4: Adaptive mesh, temperature field and pressure field for $Ra = 10^6$ and $Pr = 0.71$

4.2 Mixed and forced convection around a hot cylinder

In this problem we analyzed the effect of the buoyancy forces on the cross flow past a hot circular cylinder. We consider that the incoming flow, approaching at velocity u_0, is at temperature $T_{\min} = T_0$. The initial fluid temperature is also T_0, whilst the cylinder surface is at temperature $T_{\max} = T_0 + \Delta T$.

Three simulations have been performed. In all cases we consider $Re = 100$ and $Pr = 1$. In the first analysis we neglected the buoyancy force. Thus, the first example corresponds to a forced convection flow problem (the Richardson number is zero). The other analyses represent mixed convection flow conditions with $Ri = 0.25$; one for buoyancy aiding convection and the other for buoyancy opposing convection.

In the three simulations the initial mesh comprised 3077 finite elements, with minimum element size $h_{\min} = 0.02d$. All cases were run from $t = 0$ to $t = 99d/u_0$.

Figure 5 presents adaptive meshes and temperature fields at $t = 99d/u_0$. Referring to Fig. 5, the adaptive mesh contains 12926 elements for the $Ri = 0$ example (pure forced convection). For the mixed convection problems ($Re = 100$, $Pr = 1$ and $Ri = 0.25$), the meshes comprise 15 884 and 9437 elements for the opposing convection and for the aiding convection examples, respectively.

We computed the drag and transversal forces per unit span F_D and F_L, acting on a hot cylinder. These forces are computed from the flow field according to $F_D = -\int_{\Gamma_c} \{\mu[(\partial u/\partial y) + (\partial v/\partial x)]n_y + [2\mu(\partial u/\partial x)n_x] - pn_x\}\mathrm{d}\Gamma$ and $F_L = -\int_{\Gamma_c} \{\mu[(\partial u/\partial y) + (\partial v/\partial x)]n_x + [2\mu(\partial v/\partial y)n_y] - pn_y\}\mathrm{d}\Gamma$, where $\mathbf{n}$ is the unit normal vector at the fluid-cylinder interface Γ_c (pointing from the fluid to the interior of the cylinder). We used $x_1 = x$, $x_2 = y$, $u_1 = u$ and $u_2 = v$. The vortex shedding frequency f is obtained from the analysis of the transversal force history. It is given in non-dimensional form by the Strouhal number $St = fd/u_0$. The drag and transversal force coefficients are respectively $C_D = 2F_D/\rho u_0^2 d$ and $C_L = 2F_L/\rho u_0^2 d$. We also computed the mean Nusselt number $\langle Nu \rangle = \langle q_w \rangle d/\kappa(T_{\max} - T_{\min})$.

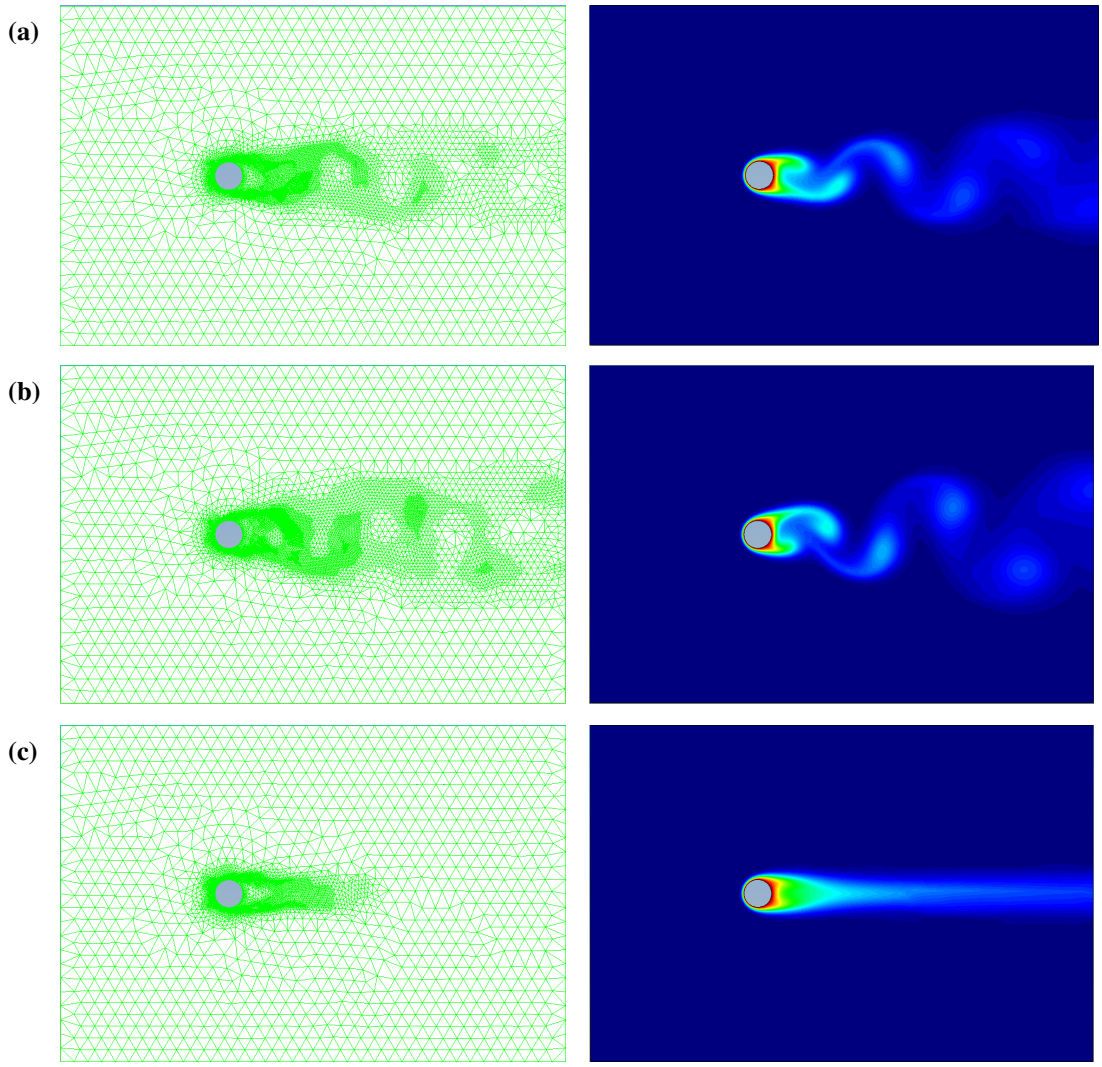

Figure 5: Cross flow past a hot cylinder with $Re = 100$ and $Pr = 1$: adaptive meshes and temperature fields $t = 99d/u_0$: (a) forced convection($Ri = 0$); (b) $Ri = 0.25$ with buoyancy opposing convection; (c) $Ri = 0.25$ with buoyancy aiding convection.

We could note that Fig. 5 also shows that the vortex shedding behavior has been suppressed in the case of buoyancy aiding convection. This is in accordance with results obtained by Patnaik *et al.* (1999).

Table 2 compares our results for the mean drag coefficient $C_{D,mean}$, the rms transversal force coefficient $C_{L,rms}$ the mean Nusselt number $\langle Nu \rangle$ and the Strouhal number (*St*) with the results provided by De Sampaio (2006).

	$C_{D,mean}$ De Sampaio (2006)	$C_{D,mean}$ **present**	$C_{L,rms}$ De Sampaio (2006)	$C_{L,rms}$ **present**	$\langle Nu \rangle$ De Sampaio (2006)	$\langle Nu \rangle$ **present**	*St* De Sampaio (2006)	***St*** **present**
$Ri = 0$	1.44	**1,40**	0.28	**0,24**	5.83	**5.80**	0.166	**0,165**
$Ri = 0.25$ buoyancy opposing convection	1.46	**1.40**	0.45	**0.39**	5.75	**5.70**	0.156	**0.154**
$Ri = 0.25$ buoyancy aiding convection	1.50	**1.50**	0	**0**	5.87	**5.86**	-	**-**

Table 2: Cross flow past a hot cylinder: comparison between the present results with De Sampaio (2006).

Note that there has been little change in the mean drag and Nusselt numbers in the three cases considered. On the other hand, the transversal force associated to the vortex shedding process is considerably more intense for the case of buoyancy opposing convection, as indicated by $C_{L,rms}$. Also note that is the case of buoyancy aiding convection the vortex shedding flow pattern disappeared. This behavior and the decrease of the Strouhal number for buoyancy opposing convection are in agreement with the results obtained by Patnaik *et al*. (1999).

5. CONCLUDING REMARKS

A second-order time accurate finite element formulation has been presented. The mass and momentum balances have been combined in a Taylor series for pressure. This is discretized in space with the Galerkin method and results in an equation suitable for computing the pressure update. Momentum balance and energy balance time-discretization are carried out with finite differences. A least square minimization of spatial residuals is performed to obtain equations for the velocity and temperature update. The proposed method introduces automatically the stabilization terms required to control wiggles in convection dominated problems and for circumventing Babuška-Brezzi restrictions on the choice of interpolating spaces for velocity and pressure. The approach leads to a partially coupled system, where pressure degrees of freedom are solved first and then the velocity and temperature degrees of freedom are computed simultaneously. The update of velocity components and temperature are obtained solving the coupled equation system shown in Equation (31).

Local time-steps for momentum and energy play the role of stabilization parameters. A simple time interpolation scheme is embedded in the method, synchronizing the time advance of the computation.

Numerical examples have been presented, covering free, forced and mixed convection flow and heat transfer. The examples shows the effectiveness of the method in stabilizing the computation of incompressible flows (mach number zero, $M = 0$). Comparison of our results with the benchmark numerical solutions and with experimental heat transfer data shows the good performance of the stabilized formulation proposed here.

6. ACKNOWLEDGEMENTS

M.F. Curi, P.A.B. de Sampaio and M.A. Gonçalves Jr. acknowledge the support of CNPq and CNEN.

7. REFERENCES

Bowyer, A., 1981. Computing Dirichlet Tessellations. Comput. J. 24, 162–166.

Brezzi, F., Fortin, M., 1991. Mixed and Hybrid Finite Element Methods. Springer, NY.

Brooks, A., Hughes, T.J.R.,1982. Streamline upwind Petrov–Galerkin formulations for convection dominated flows with particular emphasis on the incompressible Navier–Stokes equations. Comput. Met. Appl. Mech. Eng.,199–259.

De Sampaio, P.A.B., 1991. A Petrov–Galerkin formulation for the incompressible Navier–Stokes equations using equal order interpolation for velocity and pressure. Int. J. Numer. Methods Eng. 31, 1135–1149.

De Sampaio, P.A.B., 1993. Transient solutions of the incompressible Navier–Stokes equations in primitive variables employing optimal local time stepping. In: Proceedings of the 8th International Conference on Numerical Methods for Laminar and Turbulent Flow, pp. 1493–1504.

De Sampaio, P.A.B., 2005. A finite element formulation for transient incompressible viscous flows stabilized by local time-steps. Comput. Methods Appl. Mech. Eng. 194, 2095–2108.

De Sampaio, P.A.B., 2006. A stabilized finite element method for incompressible flow and heat transfer: a natural derivation based on the use of local time-steps. Comput. Methods Appl. Mech. Eng. 195 (44–47), 6177–6190.

De Sampaio, P.A.B., Coutinho, A.L.G.A., 1999. Simulation of free and forced convection incompressible flows using an adaptive parallel/vector finite element procedure. Int. J. Numer. Methods Fluids 29, 289–309.

De Sampaio, P.A.B., Gonçalves Jr., M.A., 2010. A second-order time accurate finite element method for quasi-incompressible viscous flows. Int. J. Numer. Meth. Fluids.

Hortmann, M., Peric´, M., Scheuerer, G. , 1990. Multigrid benchmark solutions for laminar natural convection flows in square cavities, in: I. Celik, C.J. Freitas (Eds.), Benchmark Test Cases for Computational Fluid Dynamics, ASME, New York, pp. 1–6.

Patnaik, B.S.V., Narayana, P.A.A., Seetharamu, K.N., 1999.Numerical simulation of vortex shedding past a circular cylinder under the influence of buoyancy, Int. J. Heat Mass Transfer, 42, 3495–3507.

Zienkiewicz, O.C., Zhu, J.C., 1987. A simple error estimator and adaptive procedure for practical engineering analysis. Int. J. Numer. Methods Eng. 24, 337–357.

8. RESPONSIBILITY NOTICE

The author M.F. Curi, P.A.B De Sampaio,. and M.A. Gonçalves Jr., are the only responsible for the printed material included in this paper.